



# Coordinated Control of the DFIG Wind Power Generating System Based on Series Grid Side Converter and Passivity-Based Controller Under Unbalanced Grid Voltage Conditions

Qiming Cheng<sup>1</sup> · Xinqiao Ma<sup>1</sup> · Yinman Cheng<sup>2</sup>

Received: 30 December 2019 / Revised: 2 June 2020 / Accepted: 8 July 2020 / Published online: 17 July 2020  
© The Korean Institute of Electrical Engineers 2020

## Abstract

In order to solve the problem of excessive damage to doubly fed induction generator (DFIG) system under the condition of unbalanced voltage, this paper presents an improved coordinated control strategy based on doubly-fed induction generator (DFIG) wind power system, which can solve these problems well. The innovation of this paper is that the parallel grid-side converter (PGSC) uses a passivity-based controller (PBC) based on the Port Control Hamiltonian Dissipation (PCHD) model. Not only can four different control goals be achieved, namely, constant voltage of DC bus voltage, grid-side active power without second harmonics, grid-side reactive power without second harmonics, and grid-side current without negative sequence component, but also to ensure that the balance of stator and rotor current without distortion, the DFIG output power and electromagnetic torque without pulsation. The proposed coordinated control strategy has the characteristics of not changing the control strategy of the rotor-side converter and avoiding complex high-order matrix. The experimental results on the software platform and the hardware platform show that the proposed coordinated control strategy has the advantages of fast response, strong anti-interference ability, high stability, less control parameters.

**Keywords** Doubly fed induction generator (DFIG) · Unbalanced voltage · Coordinated control · Series grid-side converter (SGSC) · Passivity-based controller (PBC)

## 1 Introduction

With the increasing impact of wind turbines for power system stability, it is necessary to ensure that the wind turbine can be effectively connected to the grid and provide reactive power under unbalanced voltage condition. Nowadays, doubly fed induction generator (DFIG) is widely used in many wind turbines because of its own advantages [1, 2]. However, when the power grid fails, the DFIG system will

be severely affected because the stator is directly connected to the power grid [3]. At the same time, for the rotor winding of DFIG, the negative sequence voltage has a larger slip, which will cause the rotor over-voltage and over-current [4, 5]. Since the existence of negative sequence components, it will cause the stator current unbalanced and the low harmonic current of the rotor current. And, it will also cause the active power, reactive power, electromagnetic torque and DC bus voltage to generate second harmonic pulses [6, 7]. The above problems will shorten the working life of the converter and the DC bus capacitor, and reduce its performance. Therefore, it is very urgent and meaningful to research the control strategy of DFIG power system and improve its uninterrupted operation ability under unbalanced grid voltage condition.

Recently, some enhanced operation and control schemes are investigated for DFIG systems under unbalanced grid voltage conditions. As reported in [8–10], the conventional PI regulator relies heavily on the rated parameters of the system, when the grid voltage sags or swells, the regulation performance will be greatly reduced. In ref. [11, 12],

✉ Xinqiao Ma  
J\_S\_Nexus@163.com

Qiming Cheng  
chengqiming@sina.com

Yinman Cheng  
chengyinman@Hotmail.com

<sup>1</sup> College of Automation Engineering, Shanghai University of Electric Power, Shanghai, China

<sup>2</sup> College of Electronics and Information Engineering, Tongji University, Shanghai, China

the proportional resonant (PR) control strategy is proposed, which can achieve the sinusoidal quantity without static control. However, when the AC component frequency has a slight offset, the gain will change greatly and the structure is more complex. PI and repetitive control are proposed in ref. [13], which can achieve better dynamic performance and higher steady-state accuracy. However, the presence of control coupling between the PI regulator and the repetitive controller will aggravate the distortion of grid current. A grid-side converter (GSC) control strategy of DFIG based on sliding mode variable structure under unbalanced grid voltage is introduced in ref. [14]. The system has simple structure, fast dynamic response and strong robustness, but there is a high frequency oscillation problem in the controlled quantity. In refs. [6, 15], the main and auxiliary current control systems based on the synchronous rotating frame (SRF) are used, the solution is effective, but the negative sequence current components need to be extracted, and the adjustment rate of the negative sequence current is slower than that of the positive sequence current.

The most fundamental reason for the fluctuation of the generator power and electromagnetic torque is the existence of the negative sequence and the harmonic component in the stator voltage under unbalanced grid voltage. Aiming at the above problems, this paper is organized as follows. Section 2 describes a doubly-fed wind power system based on the series grid-side converter (SGSC). This system has the advantages of stator voltage control and can achieve symmetrical and stable operation of the generator [16, 17]. The specific control targets of SGSC and parallel grid-side converter (PGSC) are designed in Sect. 3. In Sect. 4, a coordinated control of the SGSC, PGSC, and rotor-side converter (RSC) is carried out. And the control schemes for PGSC and RSC using passivity-based controller (PBC) in the positive-sequence SRF and negative-sequence SRF. Then, combines with PGSC's coordinated control to achieve the suppression to system's total output power fluctuation. The use of the passive control theory is more conducive to the global stability of the system. Finally, the simulation results in Sects. 5 and 6 intensively prove that compared with the traditional controller, the proposed method has the advantages of easier parameter adjustment, faster response speed and stronger robustness.

## 2 Operation Analysis of DFIG with SGSC Under Unbalanced Voltage Condition

Since RSC is used to eliminate the second harmonic of electromagnetic torque and stator output reactive power, the electromagnetic torque waveform is DC component without second harmonic, and the stator reactive power is also DC component without second harmonic. However, the second

harmonic of the stator output active is not zero. Because PGSC is used to offset the second harmonic of the stator output active power generated by RSC, the total output active power does not contain the second harmonic, but the total output reactive power contains the second harmonic. Therefore, the above coordinated control strategy can only meet part of the control targets of the RSC or the GSC at a time. To this end, this paper proposes to use the harmonics generated by SGSC and the second harmonic generated by PGSC to cancel each other and control the stator voltage, so as to suppress the second frequency fluctuation of the total output power of the system.

The investigated system [18] is shown in Fig. 1. In Fig. 1, the SGSC is connected to DFIG stator through a series transformer, so the DFIG stator voltage includes the output voltage of the series transformer and the grid voltage. In order to ensure that DFIG can operate normally under unbalanced grid voltage, the stator negative sequence voltage can be offset by injecting appropriate series compensation voltage into the stator loop. At the same time, in order to eliminate the influence of the leakage resistance drop on the DFIG stator voltage of the series-connected converter, it is necessary to control the SGSC to inject a positive sequence compensation voltage vector into the stator circuit and ensure that the DFIG stator voltage positive sequence component is the same as the positive voltage component of the grid voltage. Then the output control voltage vector of the SGSC can be obtained under the unbalanced grid voltage, as shown in formula (1).

$$u_{\text{series}} = u_{\text{com+}} - u_{g-} \quad (1)$$

where,  $u_{\text{series}}$  represents the series transformer output voltage vector;  $u_{\text{com+}}$  is the positive sequence voltage vector required for the SGSC, and  $u_{g-}$  is the negative sequence voltage vector of the grid. When the SGSC is controlled to make the DFIG stator voltage symmetrical, the traditional way can also be used to control the RSC and DFIG operation is not affected under the unbalanced grid voltage. Therefore, the generator set, the rotor current can be balanced and the

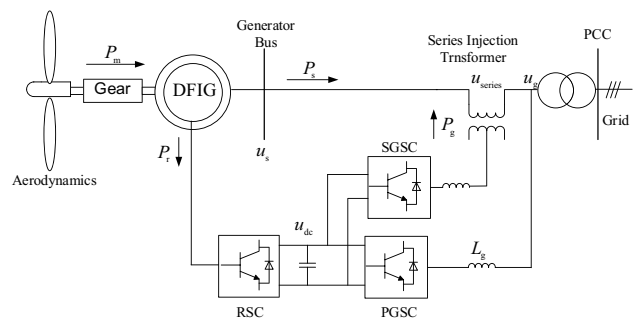


Fig. 1 Configuration of DFIG System with SGSC

motor output power and electromagnetic torque can remain stable and undisturbed. The current flowing through SGSC and series transformer will remain symmetrical. Under the action of the negative sequence voltage and the stator positive sequence current, the active and reactive power flowing through the SGSC will contain the second frequency ripple component, which will cause the whole system output active and reactive power to fluctuate. SGSC’s double octave pulsating active power will be injected into the DC side capacitor, which will cause the DC bus voltage to generate double frequency ripple.

It can be seen from Fig. 1 that PGSC and the grid are in parallel. At this time, the positive and negative sequence mathematical model of PGSC in the dq axis orthogonal coordinate system were obtained as Eqs. (2) and (3):

$$\begin{cases} L_g i_{gd+}^p = -R_g i_{gd+}^p + L_g \omega i_{gq+}^p + u_{gd+}^p - v_{gd+}^p \\ L_g i_{gq+}^p = -R_g i_{gq+}^p - L_g \omega i_{gd+}^p + u_{gq+}^p - v_{gq+}^p \end{cases} \quad (2)$$

$$\begin{cases} L_g i_{gd-}^n = -R_g i_{gd-}^n + L_g \omega i_{gq-}^n + u_{gd-}^n - v_{gd-}^n \\ L_g i_{gq-}^n = -R_g i_{gq-}^n - L_g \omega i_{gd-}^n + u_{gq-}^n - v_{gq-}^n \end{cases} \quad (3)$$

where,  $L_g$  and  $R_g$  are the equivalent inductance and resistance of the grid side circuit,  $u_{gd+}^p$ ,  $v_{gd+}^p$  and  $u_{gq+}^p$ ,  $v_{gq+}^p$  are respectively the positive sequence voltage components of the grid side and the AC side under the positive sequence dq axis.  $i_{gd+}^p$  and  $i_{gq+}^p$  are respectively the positive sequence current components of the AC side under the positive sequence dq axis.

Similarly,  $u_{gd-}^n$ ,  $v_{gd-}^n$  and  $u_{gq-}^n$ ,  $v_{gq-}^n$  are the negative sequence voltage components of the grid side and the AC side under the negative sequence dq axis.  $i_{gd-}^n$  and  $i_{gq-}^n$  are respectively the negative sequence current components of the AC side under the negative sequence dq axis.  $\omega$  is the grid angle frequency.

Equations (2) and (3) show that when the grid is unbalanced, a negative sequence current component will be generated in the PGSC, and the power flowing through PGSC will have second frequency fluctuations, as follows:

$$\begin{cases} P_g = P_{gav} + P_{gsin2} \sin 2\omega t + P_{gcos2} \cos 2\omega t \\ Q_g = Q_{gav} + Q_{gsin2} \sin 2\omega t + Q_{gcos2} \cos 2\omega t \end{cases} \quad (4)$$

where, subscript gav, gsin2 and gcos2 respectively represent the power of the DC component, the second frequency sine and cosine wave components. In other words,  $P_g$  and  $Q_g$  are the active power and reactive power on the grid side, respectively.  $P_{gav}$  and  $Q_{gav}$  are the DC components of the active power and reactive power on the grid side, respectively.  $P_{gsin2}$  and  $Q_{gsin2}$  are the second frequency sine components of the active power and reactive power on the grid

side, respectively.  $P_{gcos2}$  and  $Q_{gcos2}$  are the second frequency cosine components of the active power and reactive power on the grid side, respectively.  $\omega$  is the grid side angle frequency. When the grid frequency is 50 Hz, its value is  $100\pi$ .

In the synchronous rotation dq coordinate system, the amplitude of each component in Eq. (4) can be expressed as Eq. (5).

$$\begin{bmatrix} P_{gav} \\ P_{gsin2} \\ P_{gcos2} \\ Q_{gav} \\ Q_{gsin2} \\ Q_{gcos2} \end{bmatrix} = -\frac{3}{2} \begin{bmatrix} u_{gd+}^p & u_{gq+}^p & u_{gd-}^n & u_{gq-}^n \\ u_{gq-}^n & -u_{gd-}^n & -u_{gq+}^p & u_{gd+}^p \\ u_{gd-}^n & u_{gq-}^n & u_{gd+}^p & u_{gq+}^p \\ u_{gq+}^p & -u_{gd+}^p & u_{gq-}^n & -u_{gd-}^n \\ -u_{gd-}^n & -u_{gq-}^p & u_{gd+}^p & u_{gq+}^p \\ u_{gq-}^n & -u_{gd-}^p & u_{gq+}^p & -u_{gd+}^p \end{bmatrix} \begin{bmatrix} i_{gd+}^p \\ i_{gq+}^p \\ i_{gd-}^n \\ i_{gq-}^n \end{bmatrix} \quad (5)$$

It can be seen that in the DFIG system with SGSC, the output power of SGSC and PGSC each contains the second frequency ripple component, which will cause the entire system to output active or reactive power with a double frequency ripple component. This will endanger the safe and stable operation of the grid to a certain extent. And active power with double octave pulse are injected into the DC capacitor through the two converters, which will also bring the DC bus voltage fluctuations and reduce the stability of the DC bus voltage. Therefore, appropriate control measures should be taken to suppress the system output active power and DC bus voltage fluctuations, and improve the operation reliability of DFIG system when the voltage is asymmetric.

### 3 Control Targets

#### 3.1 Control Targets of SGSC

Based on the above analysis, it is not difficult to get the control target of SGSC under unbalanced grid voltage, that is, to make the DFIG terminal voltage always consistent with the positive sequence voltage components. This will not only eliminate the influence of negative sequence voltage on DFIG under unbalanced grid voltage, but also ensure the DFIG terminal voltage is consistent with the grid voltage. It can be expressed as (6).

$$\begin{cases} \mathbf{u}_{sdq+} = \mathbf{u}_{gdq+} \\ \mathbf{u}_{sdq-} = 0 \end{cases} \quad (6)$$

where,  $\mathbf{u}_{gdq+}$  is the positive sequence grid voltage vector,  $\mathbf{u}_{sdq+}$ ,  $\mathbf{u}_{sdq-}$  are stator positive sequence, negative sequence voltage vector.

### 3.2 Control Targets of PGSC

Through the analysis of formula (5), the grid-side converter has four control objectives, namely,

- 1) Target 1: The input current on the grid side does not contain negative sequence components ( $i_{gdq-}^n + i_{sdq-}^n = 0$ ).

Ignoring the active loss of device, line resistance and filter capacitor, combining formula (5) and solving the corresponding matrix equation, then the grid side command current value corresponding to the target 1 can be obtained. It can be expressed as Eq. (7).

$$\begin{cases} i_{gd+}^{p*} = -\frac{2}{3} \frac{u_{gd+}^p P_{seriesav} + u_{gq+}^p Q_{seriesav}}{(u_{gd+}^p)^2 + (u_{gq+}^p)^2} \\ i_{gq+}^{p*} = -\frac{2}{3} \frac{u_{gq+}^p P_{seriesav} - u_{gd+}^p Q_{seriesav}}{(u_{gd+}^p)^2 + (u_{gq+}^p)^2} \\ i_{gd-}^{n*} = i_{gq-}^{n*} = 0 \end{cases} \quad (7)$$

- 2) Target 2: The input power of the grid side contains only the DC component ( $P_{gsin2} - P_{seriesin2} = 0, P_{gcos2} - P_{seriescos2} = 0$ ).

In combination with (5), establishing and solving the matrix equation similar to the target 1, the corresponding to the grid side current reference value of target 2 can be obtained. As follows,

$$\begin{cases} i_{gd+}^{p*} = -\frac{2}{3} \left( \frac{u_{gd+}^p P_{seriesav} + u_{gq+}^p Q_{seriesav}}{D_1} + \frac{u_{gq+}^p Q_{seriesav}}{D_2} \right) \\ i_{gq+}^{p*} = -\frac{2}{3} \left( \frac{u_{gq+}^p P_{seriesav} - u_{gd+}^p Q_{seriesav}}{D_1} - \frac{u_{gd+}^p Q_{seriesav}}{D_2} \right) \\ i_{gd-}^{n*} = -\frac{2}{3} \left( -\frac{u_{gd-}^n P_{seriesav} + u_{gq-}^n Q_{seriesav}}{D_1} + \frac{u_{gq-}^n Q_{seriesav}}{D_2} \right) \\ i_{gq-}^{n*} = -\frac{2}{3} \left( -\frac{u_{gq-}^n P_{seriesav} - u_{gd-}^n Q_{seriesav}}{D_1} - \frac{u_{gd-}^n Q_{seriesav}}{D_2} \right) \end{cases} \quad (8)$$

where,  $D_1 = u_{gd+}^{p2} + u_{gq+}^{p2} - u_{gd-}^{n2} - u_{gd-}^{n2}$ ,  $D_2 = u_{gd+}^{p2} + u_{gq+}^{p2} + u_{gd-}^{n2} + u_{gd-}^{n2}$ . If the positive sequence grid voltage is oriented to the d axis, namely  $u_{gq+}^p = 0$ , then the PGSC command current value can be retrieved. Normally, the network side unit power factor control is achieved by setting  $i_{gq+}^{p*} = 0$ . It can be seen from Fig. 1, the system DC bus capacitor instantaneous power is the instantaneous power difference flowing through the RSC, SGSC and GSC. Since the RSC is still operating in a symmetrical manner, the rotor side power in the above equation can be kept stable without fluctuation, and the double frequency instantaneous power flowing through the SGSC and PGSC will cause the DC bus voltage to have a double peak ripple in the unbalanced grid. The instantaneous power of the DC bus capacitor can be expressed as (9).

$$\begin{aligned} & \frac{1}{2} C \frac{du_{dc}^2}{dt} \\ & = P_g - P_r - P_{series} \\ & = (P_{g_{av}} - P_r - P_{series_{av}}) + [\tilde{P}_g(t) - \tilde{P}_{series}(t)] \end{aligned} \quad (9)$$

where,  $\tilde{P}_g(t)$ ,  $\tilde{P}_g(t)$  and  $\tilde{P}_{series}(t)$ ,  $\tilde{P}_{series}(t)$  are the input power fluctuating component of the grid side and the series transformer, respectively.  $u_{dc}(t)$ ,  $\tilde{u}_{dc}(t)$  is the fluctuating component of DC bus voltage.

Then, the steady-state DC bus voltage  $u_{dc}$  is as follows:

$$u_{dc} = u_{dcav} + \tilde{u}_{dc}(t) = u_{dcav} + \frac{1}{2\omega} u_{dcav} [(P_{gsin2} - P_{seriesin2}) + (P_{gcos2} - P_{seriescos2})] \quad (10)$$

From Eq. (10), we can conclude that when suppressing the total output active wave fluctuations, the DC bus voltage of the second frequency fluctuations can also be effectively limited, which will help the DC bus operation and improve system reliability.

- 3) Target 3: The constant DC bus voltage ( $u_{dcsin2} = u_{dccos2} = 0$ ).

Similar steps to solve targets 1 and 2, the corresponding to the grid side current reference value of target 3 can be obtained. As follows:

$$\begin{cases} i_{gd+}^{p*} = -\frac{2}{3} \left( \frac{u_{gd+}^p P_{seriesav} + u_{gq+}^p Q_{seriesav}}{D_1} + \frac{u_{gq+}^p Q_{seriesav}}{D_2} \right) \\ i_{gq+}^{p*} = -\frac{2}{3} \left( \frac{u_{gq+}^p P_{seriesav} - u_{gd+}^p Q_{seriesav}}{D_1} - \frac{u_{gd+}^p Q_{seriesav}}{D_2} \right) \\ i_{gd-}^{n*} = -\frac{2}{3} \left( -\frac{u_{gd-}^n P_{seriesav} + u_{gq-}^n Q_{seriesav}}{D_1} + \frac{u_{gq-}^n Q_{seriesav}}{D_2} \right) \\ i_{gq-}^{n*} = -\frac{2}{3} \left( -\frac{u_{gq-}^n P_{seriesav} - u_{gd-}^n Q_{seriesav}}{D_1} - \frac{u_{gd-}^n Q_{seriesav}}{D_2} \right) \end{cases} \quad (11)$$

- 4) Target 4: The reactive power input to the grid side contains only the DC component ( $Q_{gsin2} - Q_{seriesin2} = 0, Q_{gcos2} - Q_{seriescos2} = 0$ ).

Similar to the above calculation, the target 4 can be expressed as Eq. (12).

$$\begin{cases} i_{gd+}^{p*} = -\frac{2}{3} \left( \frac{u_{gd+}^p P_{seriesav} + u_{gq+}^p Q_{seriesav}}{D_2} + \frac{u_{gq+}^p Q_{seriesav}}{D_1} \right) \\ i_{gq+}^{p*} = -\frac{2}{3} \left( \frac{u_{gq+}^p P_{seriesav} - u_{gd+}^p Q_{seriesav}}{D_2} - \frac{u_{gd+}^p Q_{seriesav}}{D_1} \right) \\ i_{gd-}^{n*} = -\frac{2}{3} \left( \frac{u_{gd-}^n P_{seriesav} - u_{gq-}^n Q_{seriesav}}{D_2} - \frac{u_{gq-}^n Q_{seriesav}}{D_1} \right) \\ i_{gq-}^{n*} = -\frac{2}{3} \left( \frac{u_{gq-}^n P_{seriesav} + u_{gd-}^n Q_{seriesav}}{D_2} + \frac{u_{gd-}^n Q_{seriesav}}{D_1} \right) \end{cases} \quad (12)$$

### 4 Control Strategy

In order to realize the stable operation of DFIG and provide transient reactive power support to the power grid during the unbalanced voltage of the grid, the SGSC can be controlled to suppress the transient DC component of the stator flux and maintain the stator voltage. Then, by controlling the PGSC to maintain the DC bus voltage constant, the optimal control target of the total output of the DFIG system is achieved. There is no fluctuation in active power or reactive power.

The control strategy of RSC is similar to PGSC’s. The outer loop uses PI control strategy and the inner loop adopts passivity-based control strategy, which not only can realize the power decoupling control of the DFIG system during the fault period, but also maximize the absorption of reactive power within the tolerances of the converter. The detailed control block diagram is shown in Fig. 2.

#### 4.1 SGSC

There is a negative sequence component of the stator flux in the asymmetrical fault of the grid voltage. Therefore, the SGSC control targets include maintaining the constant amplitude component of the generator stator voltage constant and suppressing the stator DC transient component. In addition, it also includes injecting a certain negative sequence control voltage to control the stator terminal voltage negative sequence component to zero. In order to meet the requirements of formula (6), the positive sequence voltage vector of the stator and the grid should be equal, and the stator negative sequence voltage vector should be controlled to zero. Therefore, this paper adopts a PIR controller

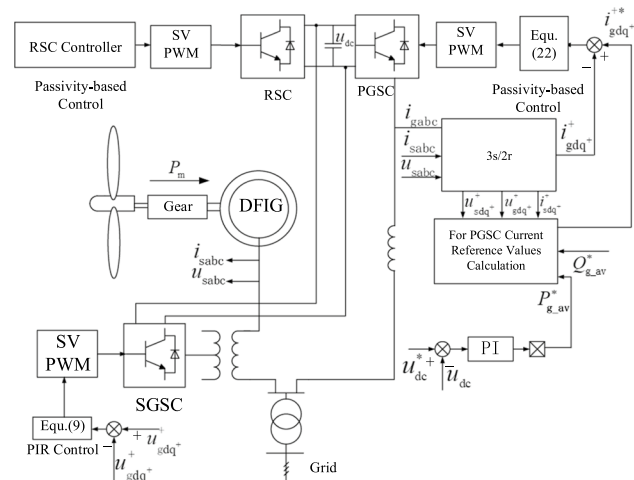


Fig. 2 Schematic diagram of the proposed control scheme for the DFIG system with SGSC

to achieve effective control of the AC component, avoid phase separation and improve the transient performance of system [19]. The transfer function can be expressed as a formula (13).

$$C_{PIR}(s) = K_p + \frac{K_i}{s} + \frac{s\omega_c K_r}{s^2 + 2\omega_c s + (\pm 2\omega_c)^2} \tag{13}$$

where,  $K_p$ ,  $K_i$ , and  $K_r$  are respectively proportional, integral coefficient, and resonant parameter.  $K_p$  and  $K_i$  play the same role as a conventional PI regulator, while the resonant compensators with  $K_r$  provides ideal gain for the AC components at the frequencies of  $2\omega$ . Practically, for a typical wind-farm grid-connected system, it is necessary to insert parameter  $\omega_c$ , called cutoff frequencies, into the resonant part to reduce its sensitivity to small frequency changes at the resonant pole.

#### 4.2 PGSC

Once the current reference is obtained for the selected control target mentioned previously, an effective current controller must be designed to regulate these currents accurately and rapidly. For this purpose, passivity-based control scheme is suggested in the paper. It is a nonlinear control theory based on the energy of the system, and is closer to the physical model of the doubly-fed machine than the traditional control strategy. It is beneficial to realize the global stability of the system. The Eq. (1) representing the mathematical model of the grid-side converter under the positive sequence synchronous dq coordinate system is rewritten as (14).

$$L_{gp} \dot{\mathbf{q}}_{gp} + C_{gp} \mathbf{q}_{gp} + \mathbf{R}_g \mathbf{q}_{gp} = \mathbf{u}_{gp} \tag{14}$$

which,  $L_{gp} = \begin{bmatrix} L_g & 0 \\ 0 & L_g \end{bmatrix}$ ,  $\mathbf{q}_{gp} = \begin{bmatrix} i_{gd}^p \\ i_{gq}^p \end{bmatrix}$ ,  $C_{gp} = \begin{bmatrix} 0 & -\omega L_g \\ \omega L_g & 0 \end{bmatrix}$ ,  $\mathbf{R}_g = \begin{bmatrix} R_g & 0 \\ 0 & R_g \end{bmatrix}$ ,  $\mathbf{u}_{gp} = \begin{bmatrix} u_{gd}^p \\ u_{gq}^p \end{bmatrix}$ .

The energy of the DFIG system is the sum of the electric energy and the mechanical energy. Therefore, its Hamiltonian function can be expressed as

$$H_{gp} = \frac{1}{2} \mathbf{q}_{gp}^T L_{gp} \mathbf{q}_{gp} \tag{15}$$

In order to establish a closed-loop expected energy function  $H_{gp}$ , it will obtain the minimum value at the point  $\mathbf{q}_{gp}^*$ , we can calculate the derivative of  $\mathbf{q}_{gp}$ , as shown in Eq. (16).

$$\dot{\mathbf{q}}_{gp} = -L_{gp}^{-1} C_{gp} L_{gp}^{-1} \frac{\partial H_{gp}}{\partial \mathbf{q}_{gp}} - L_{gp}^{-1} R_{gp} L_{gp}^{-1} \frac{\partial H_{gp}}{\partial \mathbf{q}_{gp}} + L_{gp}^{-1} \mathbf{u}_{gp} \tag{16}$$

Choose  $\mathbf{g}_{gp} = L_{gp}^{-1}$ ,  $\mathbf{J}_{gp} = -L_{gp}^{-1} C_{gp} L_{gp}^{-1}$  and  $\mathbf{R}_{gp} = L_{gp}^{-1} R_{gp} L_{gp}^{-1}$ , we can achieve the DFIG grid side posi-

tive sequence component based on the port controlled Hamilton dissipative (PCHD) model, as follow (17).

$$\begin{cases} \dot{q}_{gp} = [J_{gp} - \mathfrak{R}_{gp}] \frac{\partial H_{gp}}{\partial q_{gp}} + g_{gp} u_{gp} \\ y_{gp} = g_{gp}^T(q_{gp}) \frac{\partial H_{gp}}{\partial q_{gp}} \end{cases} \quad (17)$$

where,  $\mathfrak{R}_{gp}$  is positive semi-definite symmetric matrix,  $J_{gp}$  is the anti-symmetric matrix and interconnection structure of PCHD. The derivative of the energy function  $H_{gp}$  with respect to time as formula (18).

$$\dot{H}_{gp} = q_{gp}^T L_{gp} \dot{q}_{gp} = q_{gp}^T L_{gp} (g_{gp} u_{gp} - \mathfrak{R}_{gp} L_{gp} q_{gp}) \quad (18)$$

Then calculate the integral on both sides of the Eq. (18) at the same time, we can get the increased energy on the left side DFIG system is less than the energy provided by the right power supply, which shows that the positive sequence system of PGSC is strictly passive under unbalanced voltage.

Similarly, the PCHD model for negative sequence components in the negative rotational coordinate system can be obtained as follows,

$$\begin{cases} \dot{q}_{gn} = [J_{gn} - \mathfrak{R}_{gn}] \frac{\partial H_{gn}}{\partial q_{gn}} + g_{gn} u_{gn} \\ y_{gn} = g_{gn}^T(q_{gn}) \frac{\partial H_{gn}}{\partial q_{gn}} \end{cases} \quad (19)$$

Interconnection and damping assignment PBC (IDA-PBC) method is used when designing the controller of the PGSC. The energy function of the positive sequence system is,

$$\begin{cases} H_{gp} = \frac{1}{2} q_{gp}^T L_{gp} q_{gp} \\ H_{gpd} = \frac{1}{2} q_{gpe}^T L_{gpe} q_{gpe} \quad q_{gpe} = q_{gp} - q_{gp}^* \end{cases} \quad (20)$$

where,  $q_{gp}^* = [i_{gd+}^{p*} \quad i_{gd+}^{p*}]^T$  is the set value of the grid side current positive sequence component. According to structure conservation of the old and new, the desirable expectation of interconnection and damping matrixes are taken as,

$$J_{gpa} = L_{gp}^{-1} \begin{bmatrix} J_{11}^{gp} & -J_{12}^{gp} \\ J_{12}^{gp} & J_{22}^{gp} \end{bmatrix} L_{gp}^{-1}, \mathfrak{R}_{gpa} = \begin{bmatrix} r_1^{gp} & 0 \\ 0 & r_2^{gp} \end{bmatrix} \quad (21)$$

where,  $J_{gpa}$  is an anti-symmetric matrix,  $J_{11}^{gp}, J_{12}^{gp}, J_{22}^{gp}$  are the interconnection factors to be determined,  $\mathfrak{R}_{gpa}$  is the positive definite symmetric matrix,  $r_1^{gp}$  and  $r_2^{gp}$  are the damping coefficients to be determined, they are non-negative and are not zero at the same time.

Through the second derivative we can obtain that  $H_{gpd}$  will get minimum value at point  $q_{gp}^*$ . Thus, the DFIG grid side controller based on the PCHD model in the positive sequence can be obtained as:

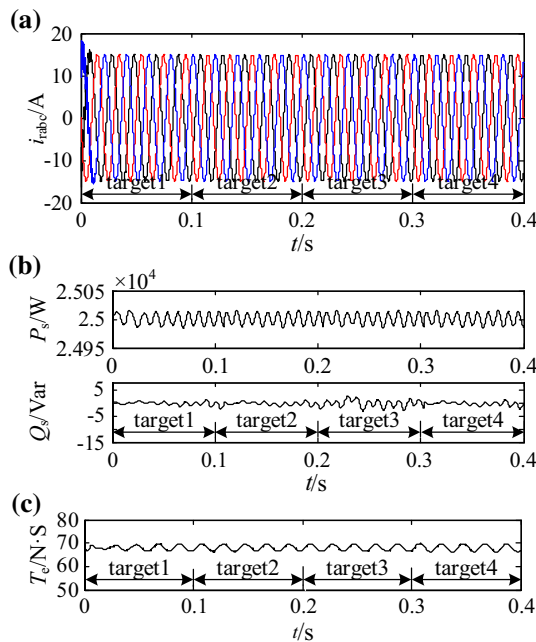


Fig. 3 Simulation results of network side selects the different control target, and the rotor side selects the control target 4

$$u_{gp} = g_{gp}^{-1} ([J_{gpa} - \mathfrak{R}_{gpa}] L_{gp} q_{gp} - [J_{gpd} - \mathfrak{R}_{gpd}] L_{gp} q_{gp}^*) \quad (22)$$

Similarly, the PCHD model for negative sequence components in the negative rotational coordinate system can be obtained as follows,

$$u_{gn} = g_{gn}^{-1} ([J_{gna} - \mathfrak{R}_{gna}] L_{gn} q_{gn} - [J_{gnd} - \mathfrak{R}_{gnd}] L_{gn} q_{gn}^*) \quad (23)$$

In formulas (21) and (22),  $J_{gpd} = J_{gp} + J_{gpa}, J_{gnd} = J_{gn} + J_{gna}$  and  $\mathfrak{R}_{gpd} = \mathfrak{R}_{gp} + \mathfrak{R}_{gpa}, \mathfrak{R}_{gnd} = \mathfrak{R}_{gn} + \mathfrak{R}_{gna}$ .

Substituting each variable expression into formulas (22) and (23), the mathematical expression of the controller based on PCHD model is:

$$\begin{cases} v_{gd+}^p = (L^2 r_1^{gp} - J_{11}^{gp}) (i_{gd+}^{p*} - i_{gd+}^p) + J_{12}^{gp} \cdot (i_{gq+}^{p*} - i_{gq+}^p) - \omega L i_{gq+}^{p*} - R i_{gq+}^{p*} + u_{gd+}^p \\ v_{gq+}^p = (L^2 r_2^{gp} - J_{12}^{gp}) (i_{gq+}^{p*} - i_{gq+}^p) - J_{12}^{gp} \cdot (i_{gd+}^{p*} - i_{gd+}^p) + \omega L i_{gq+}^{p*} - R i_{gq+}^{p*} + u_{gq+}^p \\ v_{gd-}^n = (L^2 r_1^{gn} - J_{11}^{gn}) (i_{gd-}^{n*} - i_{gd-}^n) + J_{12}^{gn} \cdot (i_{gq-}^{n*} - i_{gq-}^n) + \omega L i_{gq-}^{n*} - R i_{gq-}^{n*} + u_{gd-}^n \\ v_{gq-}^n = (L^2 r_2^{gn} - J_{22}^{gn}) (i_{gq-}^{n*} - i_{gq-}^n) - J_{12}^{gn} \cdot (i_{gd-}^{n*} - i_{gd-}^n) - \omega L i_{gq-}^{n*} - R i_{gq-}^{n*} + u_{gq-}^n \end{cases} \quad (24)$$

The control system of PGSC is shown in detail in Fig. 3, the voltage loop adopts PI control strategy and current loop adopts passivity-based control strategy.

### 4.3 RSC

For RSC, due to the DFIG terminal voltage is always symmetrical under unbalanced grid voltage, RSC can still use the traditional control strategy based on stator voltage orientation or stator flux orientation. Here, its control strategy is similar to the PGSC, the inner loop uses passivity-based control and the outer loop uses PI control strategy. Therefore, the detailed control strategy is not described here.

## 5 Simulation Results

A detailed simulation model of a 2 MW wind generator connected to the grid has been developed using Matlab/Simulink platform to study the performance of the proposed control scheme. Assuming a phase voltage drop 10%. The parameters of the system are given as follows, the parameters of the DFIG are given in Table 1; the control parameters for PIR and PI in the voltage loop of SGSC and PGSC are shown in Table 2. In order to further simplify the controller structure on the basis of ensuring the system strictly passive, in the current loop of RSC and PGSC, we choose the damping coefficient, the interconnection coefficient.

In order to illustrate the advantages of the proposed method of combining SGSC and PBC, a simulation comparison of three methods has been made in this paper, that is, the control in the text (Let’s call it SGSC + PBC), only using SGSC with PI control (Let’s call it SGSC + PI) and only use PBC control (Let’s call it PBC). During the period of  $t=0-0.4$  s, three kinds of control strategies are used to realize the operation under the unbalanced power grid. And four different control targets are realized in different time periods: 0–0.1 s, corresponding to control target 1; 0.1–0.2 s, the control target 2; 0.2–0.3 s, control target 3, and 0.3–0.4 s control target 4. The rotor side selects a control target that

**Table 2** Parameters of the GSC controllers

SGSC			PGSC	
$K_p$	$K_i$	$K_r$	$K_p$	$K_i$
10.5	50.5	2.8	0.2	30

maintains a constant electromagnetic torque to reduce the mechanical load on the wind system shaft [15].

Since the grid side and the rotor side of the DFIG can be controlled separately, when choose different targets on grid side, the control effect of maintaining a constant electromagnetic torque on the rotor side is basically unchanged. The effect of PBC on the rotor side is better than that of PI control has been discussed in many literatures, so, PBC is adopted in this paper. Simulation results are shown in Fig. 3. As shown in Fig. 3a, the rotor side current is well controlled when the grid is unbalanced. And in Fig. 3, the given control target is achieved, that is, eliminating the double harmonics of the DFIG output reactive power of stator and electromagnetic torque.

DC bus voltage waveforms under the three control strategies are shown in Fig. 4. It can be seen that under the same condition of unbalanced voltage, when selecting the control target 1, the DC bus voltage reaches a stable value at 20 ms under the SGSC + PI control strategy. Using the SGSC + PBC, it will be stable at 3 ms. Under the control target 2 to control target 4, its oscillation is small and waveform is smoother under the control strategy in this paper than the previous two strategies. Therefore, the speed of dynamic response of the control strategy mentioned in this paper is faster and the anti-interference ability is stronger.

Figure 5 shows the current waveforms on the grid side of the three control strategies. Comparatively in Fig. 5a–c, under the control of target 1, the overshoot of the grid current is larger in the 0–0.06 s under the SGSC + PI control strategy, which is easy to cause the converter to saturate. However, the PBC and the SGSC + PBC strategy have no overshoot. When selecting the control targets 2 and 3, the effects of the three control strategies are similar. In the target 4, under the first control strategy, the grid current to achieve a relatively balance

**Table 1** Simulation parameters of DFIG system

Parameters	Values
Stator resistance $R_s$	1.115 $\Omega$
Rotor resistance $R_r$	1.083 $\Omega$
Stator/rotor inductance $L_s$	0.2137 H
Magnitizing inductance $L_m$	0.2037 H
Number of pole pairs $n_p$	3
Motor rated voltage $U_s$	380 V
DC bus voltage $U_{dc}$	700 V

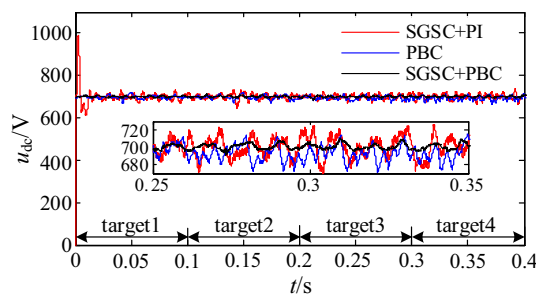


**Fig. 4** DC bus voltage waveforms by three control strategies

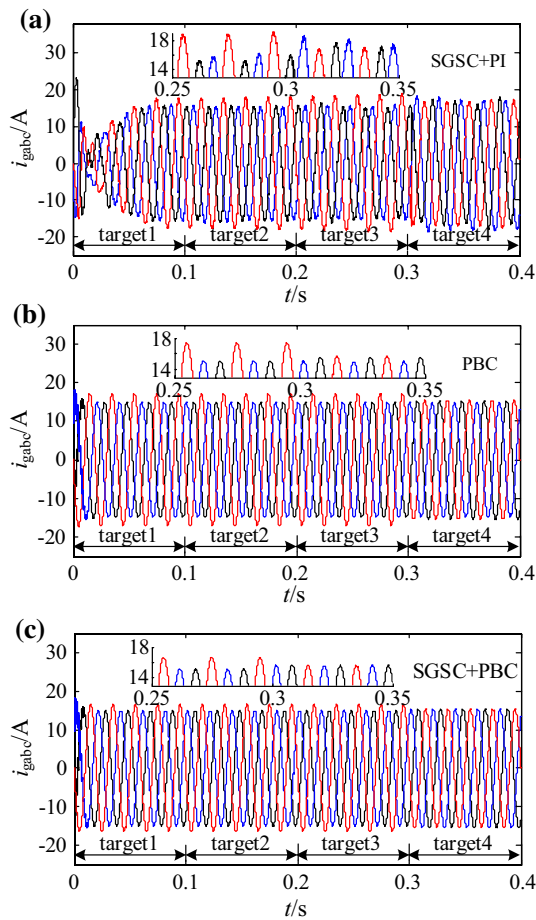


Fig. 5 Grid side current waveforms by three control strategies

at 0.35 s, the other two control strategies have been balanced when 0.3 s. However, the two-phase drop current has not fully recovered under the PBC strategy. Therefore, the control strategy mentioned in this paper has obvious advantages in dynamic response speed and stability.

Figure 6 shows the power waveforms of the grid side of the three control strategies. Table 3 shows the ratio of active and reactive twofold harmonic ripple components to average power when these strategies are used for four different control targets. It can be seen from Fig. 6 and Table 3 that under the control targets 1–4, compared with the SGSC + PI control and PBC, the active and reactive power stabilization time, overshoot and harmonic content is smaller under the proposed control strategy. Therefore, the grid side power control strategy proposed in this paper is superior to the former two control strategies in terms of control performance.

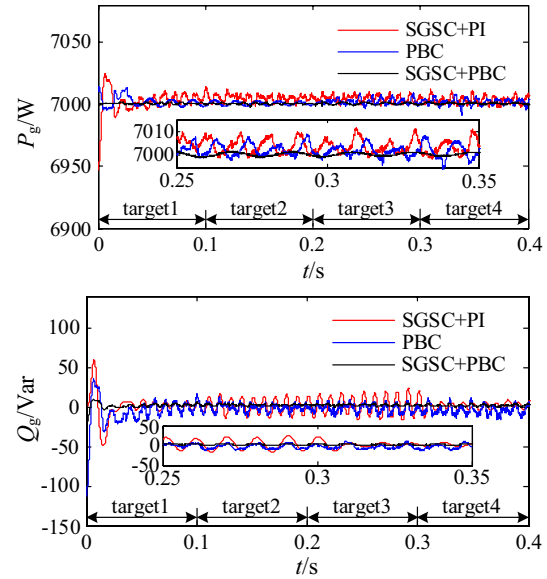


Fig. 6 Grid-side power waveforms by three control strategies

Table 3 Comparison of operation results of three control methods under different control objectives

Target	1	2	3	4
Control strategy				
SGSC+PI				
P/%	3.45	3.98	3.98	1.81
Q/%	6.32	3.31	3.31	2.65
PBC				
P/%	1.34	1.47	1.47	1.56
Q/%	1.86	0.33	0.33	1.22
SGSC+PBC				
P/%	1.05	0.69	0.69	1.03
Q/%	1.23	0.34	0.34	0.18

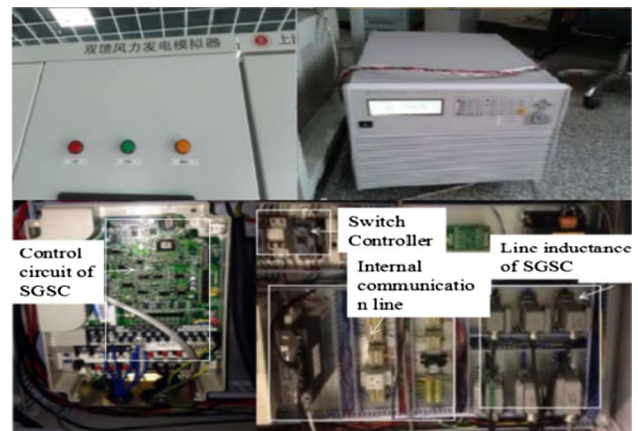


Fig. 7 Physical wiring diagram of DFIG and control system



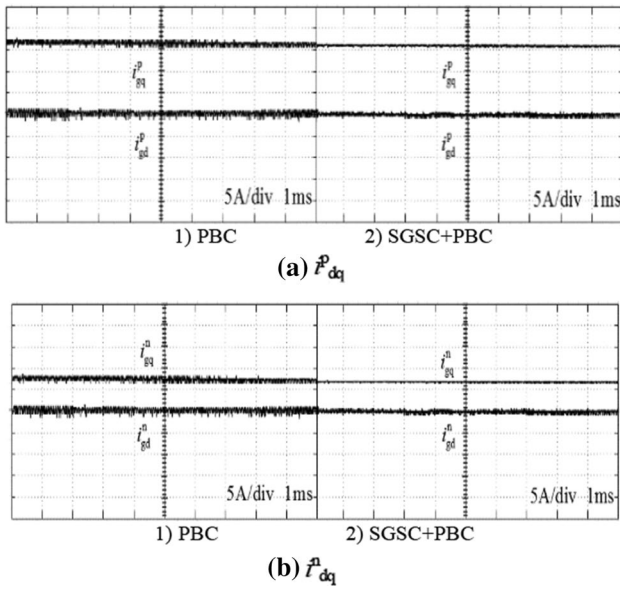


Fig. 8 Experimental results of control target 1

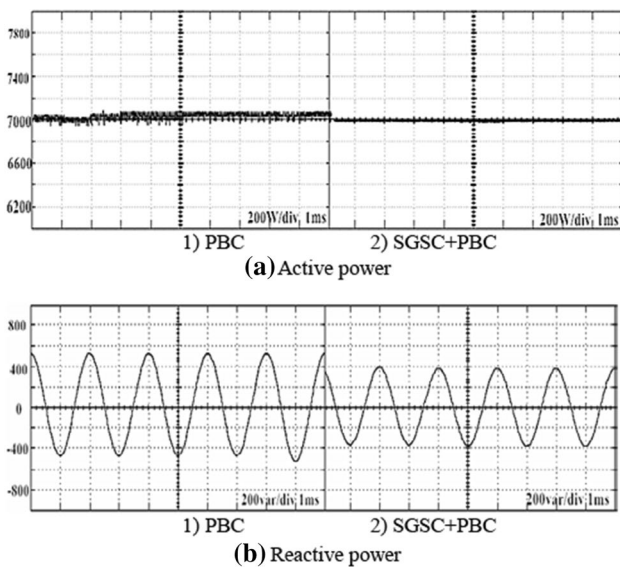


Fig. 9 Experimental results of control target 2

## 6 Experimental Result

Figure 7 shows the schematic diagram of the experimental system. The platform consists of doubly-fed generator, prime mover, SGSC, PGSC, RSC and their respective control systems. Among Which, the power switch of the converters adopt SIEMENS EUPEC 3rd generation IGBT module, IGBT drive module using CONCEPT company SCALE 2SD315AI, the grid-side and rotor-side controllers

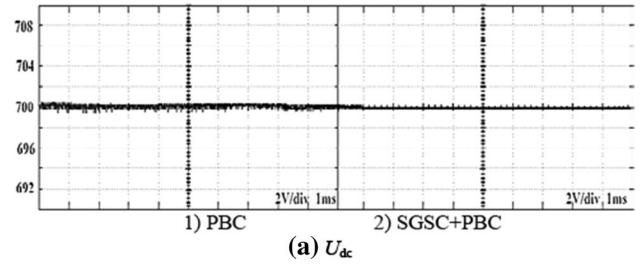


Fig. 10 Experimental results of control target 3

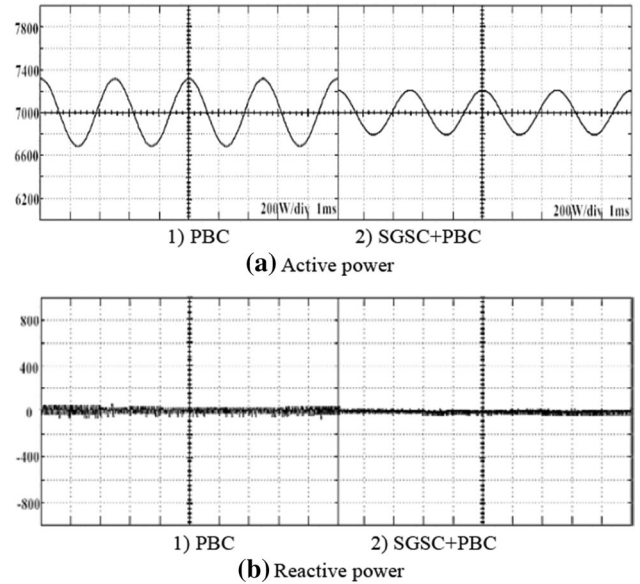


Fig. 11 Experimental results of control target 4

use TI’s DSP 28335, the wind turbine instead by the prime mover-Z4-132-3 DC motor, its rated 15 kW, rated speed 1000 rpm. The parameters of DFIG are completely consistent with the parameters in simulation. In the experiment, the grid side converter is equivalent to a resistor.

Figures 8, 9, 10, and 11 are the experimental waveforms obtained when control objectives of the grid side is chosen form target 1 to target 4 and the rotor side is selected the control target 2 [15], the PBC strategy is adopted on the left side and the control strategy in this paper is adopted on the right.

As can be seen from Fig. 8, the two control strategies under control target 1, the positive and negative current waveforms on the grid side are stable at the dq axis, that is, the grid current is sinusoidal. From Fig. 9, under the control target 2, the active power of the grid is 7 kW, and the reactive power fluctuates up and down at 0Var, which is consistent with the conclusion that the reactive power in the simulation contains the second harmonic ripple. In Fig. 10, choose the control target 3, the DC bus voltage is clearly

stable at 700 V. In Fig. 11, under the control target 4, the reactive power of the grid is a DC quantity, and the grid active power fluctuates up and down at 7 kW, and contains the second harmonic. Therefore, combining the SGSC and PBC, that is, the proposed control strategy, the fluctuations of the experimental waveforms of power, voltage and current are significantly smaller than the results obtained by the passivity-based control strategy, so the results on the experimental platform also verify the correctness and effectiveness of the control method proposed in this paper.

## 7 Conclusion

The passive control theory is a nonlinear control theory based on system energy. It is closer to the physical model of DFIG than traditional control strategies and can achieve global stability of the system. In this paper, the SGSC + PBC is compared with the SGSC + PI and PBC. Through the theoretical analysis, the software simulation and the hardware experiment, we can draw the following conclusions,

- (1) SGSC can eliminate the influence on the stator voltage control loop and suppress the system output power two-fold frequency fluctuation under unbalanced grid voltage. And the system based on passivity-based control has global stability, does not depend on some specific structural attributes of DFIG system, the parameter is easy to adjust, and the control effect is ideal;
- (2) Compared with traditional SGSC + PI control and PBC, the coordinated control strategy of SGSC + PBC proposed in this paper can make the DFIG coordinated control system have the characteristics of fast response, less parameters, easy adjustment, strong anti-interference ability and high stability.

**Acknowledgements** This work was supported by the National Natural Science Foundation of China (61573239), and Shanghai key laboratory of power station automation technology (13DZ2273800).

## References

1. Liu C, Blaabjerg F, Chen W et al (2012) Stator current harmonic control with resonant controller for doubly fed induction generator. *IEEE Trans Power Electron* 27(7):3207–3220
2. Kou P, Liang D, Li J et al (2018) Finite-control-set model predictive control for DFIG wind turbines. *IEEE Trans Autom Sci Eng* 15(3):1004–1013
3. Sun L, Xu B, Du W et al (2017) Model development and small-signal stability analysis of DFIG with stator winding inter-turn fault. *IET Renew Power Gener* 11(3):338–346
4. Nuutinen P, Peltoniemi P, Silventoinen P (2013) Short-circuit protection in a converter-fed low-voltage distribution network. *IEEE Trans Power Electron* 28(4):1587–1597
5. Li X, Zhang X, Lin Z et al (2016) Adaptive multiple MPC for a wind farm with DFIG: a decentralized-coordinated approach. *J Electr Eng Technol* 11(5):1116–1127
6. Martinez MI, Tapia G, Susperregui A et al (2012) Sliding-mode control for DFIG rotor-and grid-side converters under unbalanced and harmonically distorted grid voltage. *IEEE Trans Energy Convers* 27(2):328–339
7. Cheng P, Nian H (2015) Collaborative control of DFIG system during network unbalance using reduced-order generalized Integrators. *IEEE Trans Energy Convers* 30(2):453–464
8. Busada CA, Bahia B et al (2012) Current controller based on reduced order generalized integrators for distributed generation systems. *IEEE Trans Ind Electron* 59(7):2898–2909
9. Liao Y, Li H, Yao J et al (2011) Operation and control of a grid-connected DFIG-based wind turbine with series grid-side converter during network unbalance. *Electr Power Syst Res* 81(1):228–236
10. Suppioni VP, Grilo AP, Teixeira JC (2016) Control methodology for compensation of grid voltage unbalance using a series-converter scheme for the DFIG. *Electr Power Syst Res* 133:198–208
11. Serra FM, De Angelo CH (2017) IDA-PBC controller design for grid connected front end converters under non-ideal grid conditions. *Electr Power Syst Res* 142:12–19
12. Cong L, Li X (2020) The nonlinear equivalent input disturbance coordinated control for enhancing the stability of hydraulic generator system. *J Electr Eng Technol* 15(2):539–546
13. Parinya P, Sangswang A, Kirtikara K et al (2018) Stochastic stability analysis of the power system incorporating wind power using measurement wind data. *J Electr Eng Technol* 13(3):1110–1122
14. Pedro R, Alvaro L, Ignacio C (2011) Multiresonant frequency-locked loop for grid synchronization of power converters under distorted grid conditions. *IEEE Trans Ind Electron* 58(1):127–138
15. Wessels C, Gebhardt F, Fuchs FW (2011) Fault ride-through of a DFIG wind turbine using a dynamic voltage restorer during symmetrical and asymmetrical grid faults. *IEEE Trans Power Electron* 26(3):807–815
16. Yao J, Li H, Chen Z et al (2013) Enhanced control of a DFIG-based wind-power generation system with series grid-side converter under unbalanced grid voltage conditions. *IEEE Trans Power Electron* 28(7):3167–3181
17. Tao Y, Tang W (2018) Virtual flux and positive-sequence power based control of grid-interfaced converters against unbalanced and distorted grid conditions. *J Electr Eng Technol* 13(3):1265–1274
18. Suppioni VP, Grilo AP, Teixeira JC et al (2019) Coordinated control for the series grid side converter-based DFIG at subsynchronous operation. *Electr Power Syst Res* 173:18–28
19. Justo JJ, Bansal RC (2018) Parallel R-L configuration crowbar with series R-L circuit protection for LVRT strategy of DFIG under transient-state. *Electr Power Syst Res* 154:299–310

**Publisher's Note** Springer Nature remains neutral with regard to jurisdictional claims in published maps and institutional affiliations.

**Qiming Cheng** was born in Yancheng, Jiangsu, China. He received his B.S. degree in Physics from Suzhou University, Suzhou, China, in 1984; and his M.S. degree in Electrical Engineering from Zhejiang University, Hangzhou, China, in 1988. In 2001, he joined the Shanghai University of Electric Power, Shanghai, China. He has presided over several key scientific research projects such as a Shanghai Key Science and Technology Research Project and a Shanghai Municipal Education Commission Key Natural Fund. He is presently working as a Professor and as a Master Tutor in the College of Automation Engineering, Shanghai University of Electric Power. His current research interests include power electronics and control, which include ac machine

drives, new energy generation, microgrid control, and electric vehicle and charging station control.

**Xinqiao Ma** was born in Nanjing, Jiangsu, China. In 2018, he entered the College of Automation Engineering of Shanghai University of Electric Power to study for a master's degree. His current research interests are automation of electric power systems, power electronic control, etc.

**Yinman Cheng** female, engineer, working at Shibe power supply company of State Grid Shanghai Electric Power Company. She graduated with a master's degree in 2019 from the College of Electronics and Information Engineering of Tongji University with her research interests in automation of electric power systems, new energy power generation control, etc.